Online Feedback-based Optimization with Multi-input Direct Constraint Control ⋆

Risvan Dirza, Sigurd Skogestad

Dept. of Chemical Engineering, Norwegian Univ. of Science & Technology (NTNU), NO-7491 Trondheim, Norway, (e-mail: risvan.dirza@ntnu.no, sigurd.skogestad@ntnu.no (corresp. author)).

Abstract:
The starting point of this paper is to solve a steady-state optimization problem with simple feedback controllers using the Primal-Dual approach. However, this approach controls the constraint indirectly and on a slow time scale by manipulating the Dual variables (Lagrange multipliers). This control strategy may lead to unacceptable dynamic violations. The main contribution of this paper is to reduce the violations by introducing direct constraint control on the fast time scale using a selector. To get consistency with the steady-state optimization, we need to change the constraints in the Primal-Dual approach to involve the input used for direct constraint control. As a further refinement of this idea, we propose a multi-input direct constraint control for cases where many inputs affect the constraint value, and where pairing with a single input may lead to input rate saturation. The proposed control structure is applied to a subsea oil production network, showing that the proposed approach can minimize the dynamic violation during transient, and can achieve optimal steady-state conditions using simple feedback controllers.

Keywords: Process optimization; Scheduling, coordination and optimization; Plantwide control

1. INTRODUCTION

Real-time optimization (RTO) deals with the steady-state economic optimization of the entire plant based on a detailed process model. As input, it needs an estimate of the present state (including constraints) and as output (results from the steady state optimization), it gives setpoints to the control layer. The RTO-layer is operating at a slow time scale (often around an hour) and because disturbances may affect the operation on a faster time scale, it is desirable to put some of the optimization into the control layer, so that at least the control layer moves the inputs in the right economic direction when there are disturbances. This is the idea of feedback-optimizing control (Morari et al., 1980), which aims at translating optimization objectives into control objectives. In addition, there may be numerical problems in the RTO-layer, especially when the model is large and complex (Wenzel et al., 2016). It may therefore be desirable to decompose the optimization problem into smaller subproblems. Decomposition may have other advantages, such as simplifying tuning and making it possible to have subparts of the optimization on a faster time scale. It may also make it possible to introduce feedback as a "trick" for numerically solving the optimization, which may make it possible to use constraint measurements more directly in the optimization layer. A comprehensive review of RTO as a feedback control problem is given by (Krishnamoorthy and Skogestad, 2022).

⋆ The authors gratefully acknowledge the financial support from SUBPRO, which is financed by the Research Council of Norway, major industry partners and NTNU.

In this paper, the starting point is that a constrained optimization problem can be translated into an unconstrained optimization problem using Lagrangian/Dual relaxation (see Krishnamoorthy (2021); Dirza et al. (2021); Krishnamoorthy and Skogestad (2022), and Fig. 1). Structurally, this method has two types of controllers, namely, a gradient controller and a central constraint controller. The gradient controller is responsible to regulate the estimated gradient of the Lagrange function, which is a function of Lagrange multipliers. To satisfy the necessary condition of optimality (NCO), this estimated gradient must be controlled to 0. To estimate the gradient, Dirza et al. (2021) uses feedback-based RTO in a distributed fashion. Hence, it is also known as distributed FRTO. The central constraint controller control the measured constraint, but the effect on the inputs are only indirect by manipulating the Lagrange multipliers. Consequently, significant dynamic violations may occur during the transient. One method that controls the active constraint directly is regional-based control as described in Jäschke and Skogestad (2012). This method works well in a small system but is problematic in a complex and large process system.

Fig. 2 illustrates the effect of direct and indirect constraint control on constrained variables during the transient. Even though it only occurs during transient, it is necessary to apply back-off when we have 'critical' hard constraints. For example, in most process system, hard constraints exist in many areas related to safety systems. If a hard constraint is violated, then the safety system must take over. A more specific example is a rupture disk (also known as a pressure safety disk). A rupture disk is a type of sacrificial part

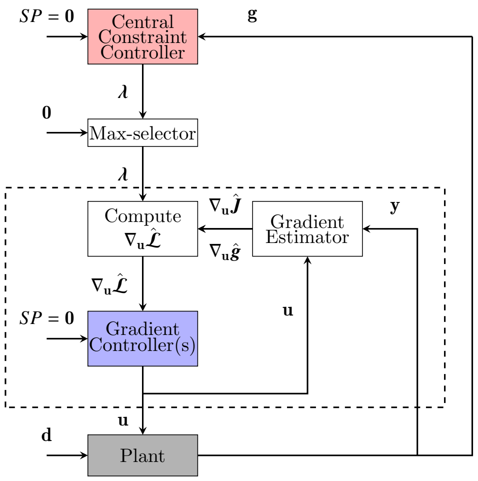

Fig. 1. Block diagram of original primal-dual scheme (Krishnamoorthy, 2021; Dirza et al., 2021). The gray box represents a given plant. The white boxes represent computational blocks. The red and blue boxes represent controller blocks with different timescales. The symbol of hat $(\hat{\cdot})$ represents estimated values, and $\mathbf{y}$ denotes the measurement set (output variables). The remaining notations are explained in Section 2

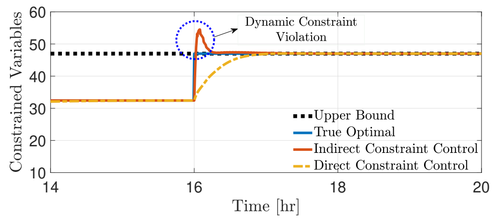

Fig. 2. The illustrated responses of constrained variables with direct and indirect constraint control.

because it has a one-time-use membrane and once the disk has ruptured it will not reseal. Since the disc is part of a protection system, it is necessary to replace it. In the context of production optimization, it is undesirable to do the replacement too often as it can lead to production performance degradation during those activities. Then, a back-off is introduced.

Applying too large back-off may lead to a significant economic penalty in the long run. Thus, we want to reduce the back-off. One solution that can reduce it, due to dynamic violation, is by directly controlling the active constraint tightly by manipulating the physical inputs, i.e., valve opening rate. However, the saturation of this input rate will interfere with the upper optimization layer (central constraint controller).

The main goal of this paper is to overcome the input rate saturation issue in minimizing the dynamic violation during transient, in the framework of primal-dual, using multi-input direct constraint control.

This paper is organized as follows. Section 2 describes the problem formulation of primal-dual with direct constraint control. Section 3 presents the proposed control structure of multi-input with direct constraint control. Section 4 compares the performance of the proposed control structure, the one with single direct constraint control, the one without direct constraint control, and the true optimal steady-state condition for a large-scale subsea oil production system before concluding the paper in Section 5.

2. PROBLEM FORMULATION

2.1 Steady-state Optimization Problem

Consider a steady-state optimization problem

$$\min_{\mathbf{u}} \quad J(\mathbf{u}, \mathbf{d}) \tag{1a}$$
$$\text{s.t.} \quad \mathbf{g}(\mathbf{u}, \mathbf{d}) \leq 0, \tag{1b}$$
$$\mathbf{u} \in \mathcal{U} \tag{1c}$$

where $\mathbf{u} \in \mathbb{R}^{n_\mathbf{u}}$ are the set of manipulated variables (physical inputs/primal variables), $\mathbf{d} \in \mathbb{R}^{n_d}$ denotes the set of parameters/disturbances, $J : \mathcal{U} \times \mathbb{R}^{n_d} \to \mathbb{R}$ is the cost function, $\mathbf{g} : \mathcal{U} \times \mathbb{R}^{n_d} \to \mathbb{R}^{n_\mathbf{g}}$ denotes the constraints. For simplicity, state $\mathbf{x}$ is not explicitly shown in problem (1).

2.2 Primal-Dual

To solve problem (1), the control structure of Primal-Dual has two layers of controllers as illustrated in Fig. 1. This section briefly explains those controllers.

Central Constraint Controller: Considering $\boldsymbol{\lambda}$ as dual variables/lagrange multipliers, the Lagrangian of Problem (1) is as follows.

$$\mathcal{L}(\boldsymbol{\lambda}, \mathbf{u}, \mathbf{d}) = J(\mathbf{u}, \mathbf{d}) + \boldsymbol{\lambda}^\top \mathbf{g}(\mathbf{u}, \mathbf{d}) \tag{2}$$

When constraint $\mathbf{g}$ is active, we assign central constraint controller to drive $\mathbf{g} \to \mathbf{0}$ by manipulating the associated dual variables $\boldsymbol{\lambda}$.

Note that, according to the KKT conditions (complementary slackness and dual feasibility), $\boldsymbol{\lambda} \geq 0$ must hold for inequality constraints in problem (1). This requirement is ensured by using a `max` operator.

This structure indicates that the presence of a central constraint controller enables automatic active constraint changing. Thus, this method is flexible in the presence of active constraints changing.

Gradient Controller: Given eq. (2) and estimated steady-state gradient of cost and constraint, then the gradient of the Lagrangian function is as follows.

$$\nabla_\mathbf{u} \mathcal{L}(\mathbf{u}, \mathbf{d}, \boldsymbol{\lambda}) = \nabla_\mathbf{u} J + \nabla_\mathbf{u}^\top \mathbf{g} \boldsymbol{\lambda} \tag{3}$$

As can be seen in eq. (3), the gradient of the Lagrangian is a function of Lagrange multipliers.

According to François et al. (2005), it is necessary to control the gradient of the Lagrangian function to 0 ($\nabla_\mathbf{u} \mathcal{L}(\mathbf{u}, \mathbf{d}, \boldsymbol{\lambda}) \to \mathbf{0}$) to satisfy the stationary condition of the necessary condition of optimality (NCO). Thus, we can consider the gradient of the Lagrangian function as self-optimizing controlled variables, and gradient controller is used to control $\nabla_\mathbf{u} \mathcal{L}(\mathbf{u}, \mathbf{d}, \boldsymbol{\lambda}) \to \mathbf{0}$.

Drawback: First, the use of single-loop (diagonal) controllers for the two controllers, assuming that we have weakly interactive systems. This is satisfied for our case study in Section 4. Second, the constraint is controlled at a slow time scale. This condition may lead to a significant dynamic violation during the transient. When we consider a hard constraint, applying any available back-off strategy, such as Galvanin et al. (2009), is usually necessary, in practice, to ensure that the overshoot does not violate the constraint significantly.

Defining $\boldsymbol{\zeta}$ as the matrix of the back-off parameter, and considering active hard constraints, then the profit loss scale is linear with the back-off parameter. Mathematically, this can be expressed as $Loss = -\boldsymbol{\lambda}^\top \boldsymbol{\zeta}$. By controlling the active hard constraints tightly, we can minimize the back-off parameter, hence reducing the profit loss in the long run. The back-off parameter can be determined based on the magnitude of the dynamic violation. Thus, reducing dynamic violations is essential to reduce economic penalties in the long run.

2.3 Primal-Dual with Direct Constraint Control

Recent solution: One possible method to minimize dynamic violation is to combine direct constraint control with the Primal-Dual framework. As opposed to the original primal-dual, appear where the constraint is indirectly controlled by central constraint controller in slow time scale, Dirza et al. (2022) suggested to control the constraint directly in fast time scale using direct constraint control. This strategy provides an alternative input to satisfy the constraint better during transient. Meanwhile, the central constraint controller is responsible to ensure that both calculated input from direct constraint controller and gradient controller are equal in steady-state.

The problem: The main assumption of this method is that the single controlled valve, that manipulates the single input used for direct constraint control, is sufficiently large and has no input rate saturation. However, the action of the single-input may be insufficient due to this saturation. Therefore, it is necessary to incorporate more available inputs to address this issue.

3. PROPOSED CONTROL STRUCTURE

In this paper, we propose to use multi-input direct constraint control structure (see, Fig. 3) to reduce the dynamic constraint violation of the original Primal-Dual structure.

In single direct constraint control (Dirza et al., 2022), a single input is assigned to control an active constraint. Meanwhile, in the proposed structure, we have multiple inputs jointly controlling the constraint directly in the fast time scale.

Multi-input direct constraint control: For direct constraint control, we need to select (pair) one combined input ($\mathbf{u}^c$) for each constraint,

$$\mathbf{u}^c = \mathbf{H}^{c\top} \mathbf{u}_{ind} \tag{4}$$

where $\mathbf{u}_{ind} \in \mathbb{R}^{n_\mathbf{u}}$ denotes the vector of all inputs provided by gradient controllers.

If we have only one constraint and select a single input, then $\mathbf{H}^c$ is a row vector with 0's except for a 1 (non-zero) for the selected input. For the multivariable case, it is reasonable to select inputs with a large effect on the constraints. A good choice is then,

$$\mathbf{H}^c = \nabla_\mathbf{u} \mathbf{g}_\mathbb{A} \tag{5}$$

where $\mathbf{H}^c \in \mathbb{R}^{n_\mathbf{u} \times n_{\mathbf{g}_\mathbb{A}}}$, $n_{\mathbf{g}_\mathbb{A}}$ is the number of constraints that we want to control tightly when they are active simultaneously, and $\nabla_\mathbf{u} \mathbf{g}_\mathbb{A}$ is the gradient of the constraints that are active simultaneously with respect to the input. However, we should put less weight on inputs that are close to their constraints, and also put less weight on inputs that have a large effective delay to the corresponding constraint. For example, we may choose,

$$\mathbf{H}^{c\top} = \begin{bmatrix} \nabla_{u_1} g_1 & \nabla_{u_2} g_1 & 0 & 0 \\ 0 & 0 & \nabla_{u_3} g_2 & \nabla_{u_4} g_2 \end{bmatrix}$$

where the first two inputs are assigned to jointly control constraint g_1, and the last two to constraint g_2. This means that the selection matrix $\mathbf{H}^c$ allows a configuration where a constraint can be directly controlled by multiple inputs.

Combining fast constraint controllers: Given $\mathbf{u}_{ind} \in \mathbb{R}^{n_\mathbf{u}}$, we can calculate the input $\mathbf{u}$ that we want to implement on the plant as follows,

$$\mathbf{u} = \mathbf{u}_{ind} + \left(\mathbf{H}^{c\dagger}\right)^\top \Delta \mathbf{u}^c \tag{6}$$

where $\mathbf{H}^{c\dagger} \in \mathbb{R}^{n_{\mathbf{g}_\mathbb{A}} \times n_\mathbf{u}}$ is the pseudo inverse of $\mathbf{H}^c$, and $\Delta \mathbf{u}^c$ labels the correction factor computed as follows,

$$\Delta \mathbf{u}^c = \left(\min\left(\mathbf{u}^c_{dir}, \mathbf{H}^{c\top} \mathbf{u}_{ind}\right) - \mathbf{H}^{c\top} \mathbf{u}_{ind}\right) \tag{7}$$

where $\mathbf{u}^c_{dir} \in \mathbb{R}^{n_{\mathbf{g}_\mathbb{A}}}$ is the input obtained from direct constraint controller.

Note that in Eq. (7), we choose a `min` selector because we assume that the more input we give, the closer the constrained variables are to the constraints. On the contrary, we would choose a `max` selector, if the input-constrained variables response is in the opposite direction.

Outer/Upper Layer: To get consistency between the direct constraint controller $\mathbf{u}^c_{dir}$ and the gradient controller $\mathbf{u}_{ind}$, the constraint $\mathbf{g} \leq \mathbf{0}$ in the outer/upper layer is replaced by the constraint $\mathbf{H}^{c\top} \mathbf{u}_{ind} \leq \mathbf{u}^c_{dir}$. Thus, in the outer/upper layer, the central constraint controller is responsible to ensure they are equal in steady state $\left(\mathbf{H}^{c\top} \mathbf{u}_{ind} - \mathbf{u}^c_{dir}\right) \to \mathbf{0}$.

4. SIMULATION RESULTS

In this section, we apply the multi-input direct constraint control on gas-lifted oil production network with $N = 6$ wells as shown in Fig. 4, which is similar to the one used in Dirza et al. (2022).

The oil production from each well, labeled by $w_{po,i}$, is manipulated by the gas-lift injection rate $w_{gl,i}$ (Note that, $\mathbf{u} = \mathbf{w}_{gl}$). The gas resource used for the gas-lift is shared and limited by available power for the gas-lift compressor, Pow^{max}_{gl}. In addition, the capacity handling for the total produced gas is limited to a maximum supply of w^{max}_{pg}. The objective of the production optimization problem is to optimally allocate the shared gas lift such that the profit is maximized. Thus, the optimization problem is

$$\min_{w_{gl,i}, \forall i \in N} \quad J_N = -\sum_{i \in N} \$_{o,i} w_{po,i} + \sum_{i \in N} \$_{gl,i} w_{gl,i} \tag{8a}$$

$$\text{s.t.} \quad \mathbf{g}(\mathbf{u}, \mathbf{d}) =: \begin{bmatrix} Pow_{gl} - Pow^{max}_{gl} \\ \sum_{i \in N} w_{pg_i} - w^{max}_{pg} \end{bmatrix} \leq 0 \tag{8b}$$

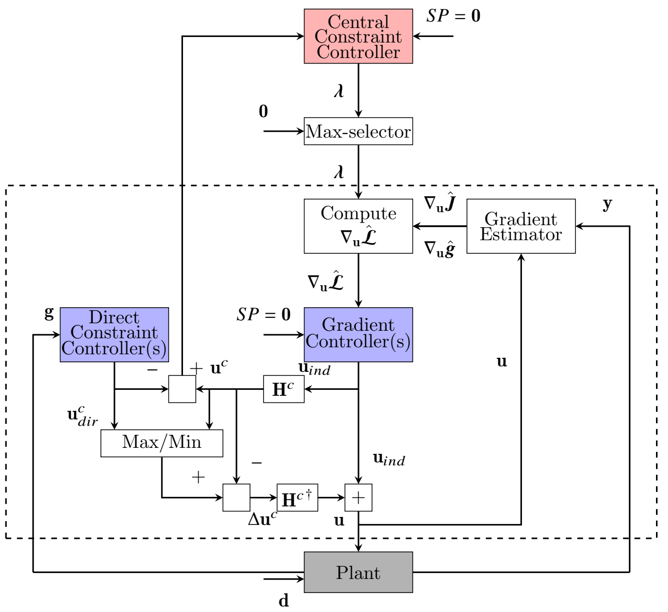

Fig. 3. Block diagram of proposed control structure with direct constraint control.

where $\$_{o,i}$ and $\$_{gl,i}$ are the oil prices and the cost of gas compression to lift the gas, respectively. The total produced gas is defined as $R_{pg_N} = \sum_{i \in N} w_{pg_i}$.

In addition, it is also normal that valves have input rate constraint. Thus, we define the input rate constraint.

$$\Delta w_{gl}^{min} \leq \Delta w_{gl,i} \leq \Delta w_{gl}^{max}, \; i = 1, ..., N$$

where, Δw_{gl}^{min} and Δw_{gl}^{max} are the lower and upper bound of the inputs rate, respectively.

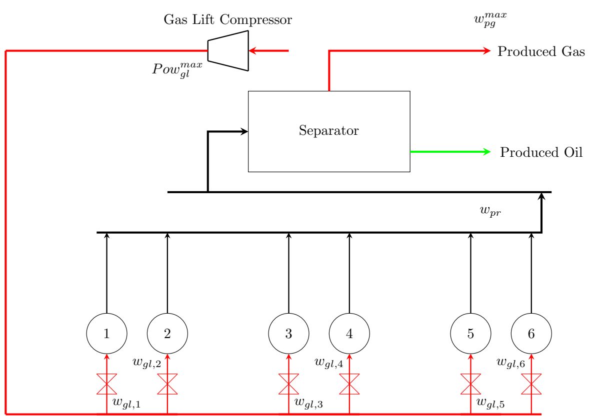

Fig. 4. A simplified process diagram of a gas-lift optimization problem with limited available power for gas-lift compressor, and limited produced gas due to maximum capacity of gas handling facility.

The gas-oil ratio (GOR), which is a reservoir property, is assumed to be varying with time (disturbances) for the different wells. Wells with a high GOR have a lighter fluid column, and hence do not require a lot of gas-lift injection compared to wells with a low gas-oil ratio. Consequently, changes in the gas-oil ratio significantly affect the optimal allocation of gas-lift injection. The available power for the gas-lift compressor is also assumed to be varying with time due to changing power load balance in the processing facility. In addition, the total produced gas is limited by the maximum capacity handling of the gas processing facility. This limit is also assumed to be time-varying.

To maintain the focus of this work, we compare the performance of the following approaches: (C1) The ideal steady-state optimal; (C2) Primal-Dual (No direct constraint control); (C3) Primal-Dual with single-input direct constraint control; (C4) The proposed control structure (multi-input direct constraint control).

To obtain the ideal steady-state optimal solutions (C1), we solve problem (8) every 150 seconds. To solve problem (8) using original Primal-Dual (C2), one can read Dirza et al. (2021) and the control structure is illustrated in Fig. 1.

The single input approach (C3) is a special case of the multi-input approach. We choose to assign $w_{gl,2}$ as the only input that is responsible for tightly controlling active constraint Pow_{gl} to Pow_{gl}^{max}, and $w_{gl,5}$ as the only input that is responsible for tightly controlling active constraint R_{pg_N} to w_{pg}^{max}. Defining g_1, and g_2 as the first and second row of $\mathbf{g}$, these pairings can also be described in matrix formulation, where matrix $\mathbf{H}^c$ is chosen as follows.

$$\mathbf{H}^{c\top} = \begin{bmatrix} 0 & 1 & 0 & 0 & 0 & 0 \\ 0 & 0 & 0 & 0 & 1 & 0 \end{bmatrix}$$

In multi-input control structure (C4), we choose $\mathbf{H}^{c\top} = \nabla_{\mathbf{u}}^{\top}\mathbf{g}_{\mathbb{A}}$. Thus, no single input, $w_{gl,i}$, is assigned to each active constraint for direct constraint control. However, there are calculated inputs, i.e., $w_{gl,pow_{gl},dir}$ and $w_{gl,w_{pg},dir}$, which are used to adjust all the inputs, labeled by $\mathbf{w}_{gl}$, if any of those constraints is active.

In this case, the two constraints (8b) are never active simultaneously. Thus, we assign all available inputs to tightly control the active one. In this case, the selected correction factor is

$$\Delta\mathbf{w}_{gl} = \min\left(\Delta\mathbf{w}_{gl,pow_{gl}}, \Delta\mathbf{w}_{gl,w_{pg}}\right)$$

where $\Delta\mathbf{w}_{gl,pow_{gl}}$ and $\Delta\mathbf{w}_{gl,w_{pg}}$ are the correction factors when g_1 and g_2 are active, respectively. The selection matrices are $\mathbf{H}^c = \nabla_{\mathbf{w}_{gl}}^{\top} g_1$ to calculate $\Delta\mathbf{w}_{gl,pow_{gl}}$, and $\mathbf{H}^c = \nabla_{\mathbf{w}_{gl}}^{\top} g_2$ to calculate $\Delta\mathbf{w}_{gl,w_{pg}}$.

To determine $\boldsymbol{\lambda}$, we use a PI controller as a central constraint controller with a max selector that gives $\boldsymbol{\lambda} = \mathbf{0}$ when the constraint is no longer optimally active. The anti-windup is necessary to avoid $\boldsymbol{\lambda}$ keeps changing in this case. Thus, this selector gives a value of either 0 or $\hat{\boldsymbol{\lambda}}$.

$$\hat{\boldsymbol{\lambda}} = \boldsymbol{\lambda}^k + \boldsymbol{K_P}\left(\mathbf{H}^{c\top}\mathbf{w}_{gl,ind} - \mathbf{w}_{gl,dir}\right)^k$$
$$+ \sum_{\tau=k-1}^{k}\left(K_I\left(\mathbf{H}^{c\top}\mathbf{w}_{gl,ind} - \mathbf{w}_{gl,dir}\right)^{\tau} + K_{aw}\left(\boldsymbol{\lambda} - \hat{\boldsymbol{\lambda}}\right)^{\tau}\right)$$

where k is the current step. K_P, K_I, and K_{aw} are proportional, integral and anti wind-up gain, respectively.

To estimate the steady-state gradients in (3) and (5), we use the model-based gradient estimation framework proposed in Krishnamoorthy et al. (2019). Note that the proposed framework is not restricted to this gradient estimation approach, so one may instead use any other model-based or model-free gradient estimation scheme (Srinivasan et al., 2011).

PID controllers are tuned using the SIMC tuning method introduced by Skogestad (2003). The local gradient controllers, the central constraint controller, and the direct constraint controller are designed with a sampling time of 1 sec.

The plant simulator is developed using the `CasADi ver. 3.5.1` toolbox (Andersson et al. (2019)) in `MATLAB R2019b`, and is simulated using the `IDAS` integrator. The simulations are performed on a `2.11 GHz` processor with `16 GB` memory for 66 hours simulation time. The GOR for all wells vary as shown in Fig. 5, where it can be seen that the system is frequently subject to disturbances, and a dramatic drop occurs at $t = 6$ hr. The available power for the gas-lift compressor (Pow_{gl}^{max}) and gas processing capacity (w_{pg}^{max}) also varies, which affects the optimal allocation of the gas-lift.

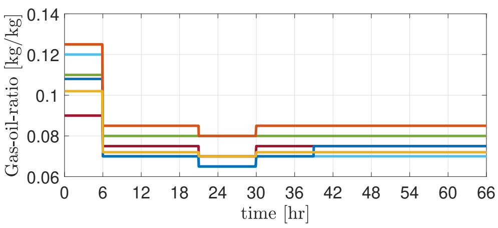

Fig. 5. GOR variations (disturbances) in the six wells.

Fig. 6 shows the simulation results comparing the ideal optimum, single-input, and the proposed control structure, where we can notice that after a dramatic GOR drop at $t = 6$ hr, more power is required by the gas-lift compressor to supply more lift gas. Thus, the maximum available power constraint is active. Note that the single-input approach does not work 'properly' to control the constraint during the transient due to input rate saturation. On the other hand, the multi-input approach can control the active constraint tightly. In addition, when the maximum gas handling capacity drops and GOR of well 1 increases at $t = 39$ hr, the active constraint region switches, and the maximum gas handling capacity is active. Without changing the control structure, the multi-input approach can automatically switch its 'mode'. After switching, this approach tightly controls the new active constraint. We can also notice that there is no significant dynamic violation in this case, so that the back-off parameters are relatively small, which means reducing more potential loss.

Fig. 7 shows that probably the only issue of multi-input (in this case) is the overshoot of dual variables at $t = 6$ hr, that appears due to disturbance and the presence of multi-input direct constraint control itself. Regarding active constraint switching, Fig. 7 (b) indicates that both single-input and multi-input can minimize dynamic violation at $t = 39$ hr with a relatively short transient time. Meanwhile, original primal-dual consumes more transient time for switching.

Finally, Fig. 8 compares and confirms that the proposed control structure is the approach that can address the issue of input rate saturation indicated by its capability to reach the optimal-steady state condition, and minimize the back-off.

Regarding economic loss due to back-off, one can notice in Fig. 6(c) that primal-dual (without direct constraint control) needs to apply around 3.2 MW of back-off of the real Pow_{gl}^{max}, single-input around 1.1 MW, and multi-input almost 0 MW in this case. This back-off has included the violation shown in Fig. 6(d) because the change of the cost shown in Fig. 8(a) of the second constraint is less than the first one. After implementing back-off strategy, both primal-dual, and single-input lose around \$369/hr, and \$104/hr, respectively. Meanwhile, the multi-input approach loses almost \$0/hr in this case.

Note that, when we assume that both constraints (8b) may be active simultaneously, we could split the inputs, i.e., the first three inputs may be used to control the first constraint tightly, and the last three may be used to the second constraint. One possible option of the selection matrix for this formulation is

$$\mathbf{H}^{c\top} = \begin{bmatrix} \nabla_{w_{gl,1}} g_1 & \nabla_{w_{gl,2}} g_1 & \nabla_{w_{gl,3}} g_1 & 0 & 0 & 0 \\ 0 & 0 & 0 & \nabla_{w_{gl,4}} g_2 & \nabla_{w_{gl,5}} g_2 & \nabla_{w_{gl,6}} g_2 \end{bmatrix}$$

and it is not necessary to select the correction factor as both of the selection factors are required by the assigned inputs. To the end, this approach provides flexibility in constructing the control structure that can satisfy any possible active constraints region/combination.

5. CONCLUSION

In this paper, we proposed a multi-input direct constraint control that is combined with primal-dual framework. We showed that the proposed control structure can overcome the issue of input rate saturation by introducing an online correction factor for the assigned inputs. Since the correction factor is constructed by a selection matrix, several inputs may jointly contribute to 'directly' controlling the active constraint, thus, avoiding the dependency on a single input. This strategy enables system-wide optimal operation with minimum back-off even under saturated inputs rate conditions, and without losing the flexibility of active constraint switching.

REFERENCES

Andersson, J., Gillis, J., Horn, G., Rawlings, J., and Diehl, M. (2019). Casadi - a software framework for nonlinear optimization and optimal control. *Mathematical Programming Computation*, 11, 1–36.

Dirza, R., Skogestad, S., and Krishnamoorthy, D. (2021). Optimal resource allocation using distributed feedback-based real-time optimization. *IFAC-PapersOnLine*, 54(3), 706–711.

Dirza, R., Skogestad, S., and Krishnamoorthy, D. (2022). Primal-dual feedback-optimizing control with direct constraint control. *14th International Symposium on Process Systems Engineering*, (in press).

François, G., Srinivasan, B., and Bonvin, D. (2005). Use of measurements for enforcing the necessary conditions of optimality in the presence of constraints and uncertainty. *Journal of Process Control*, 15(6), 701–712.

Galvanin, F., Barolo, M., Bezzo, F., and Macchietto, S. (2009). A backoff strategy for model-based experiment design under parametric uncertainty. *AIChE Journal*, 56(8), 2088–2102.

Jäschke, J. and Skogestad, S. (2012). Optimal controlled variables for polynomial systems. *Journal of Process Control*, 22(1), 167–179.

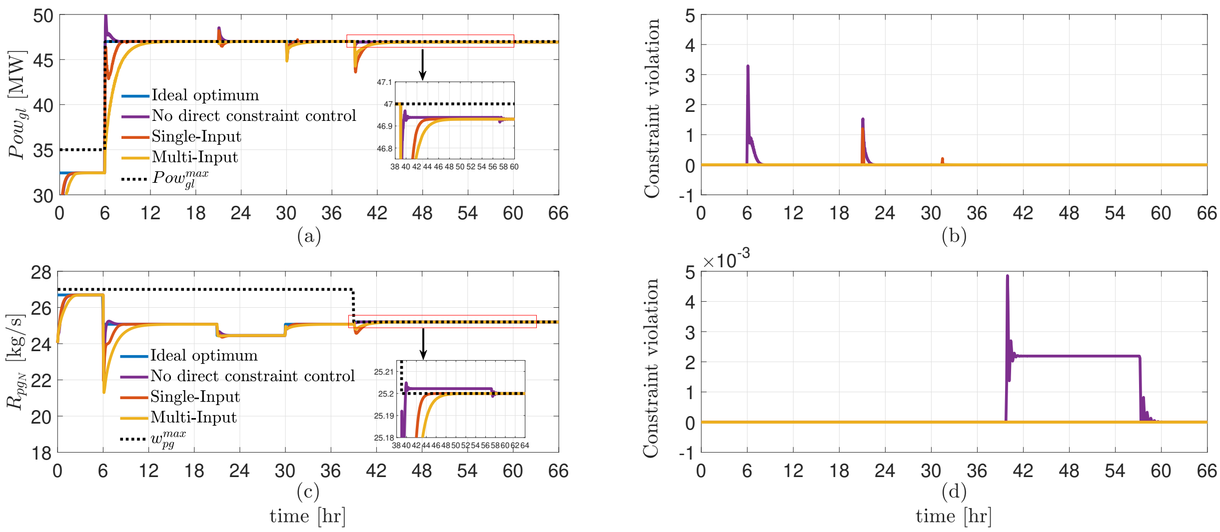

Fig. 6. Simulation results showing the constraint tracking and control performance of the multi-input approach compared to single-input, primal-dual and ideal optimum, along with the error to the ideal one (right-hand plots)

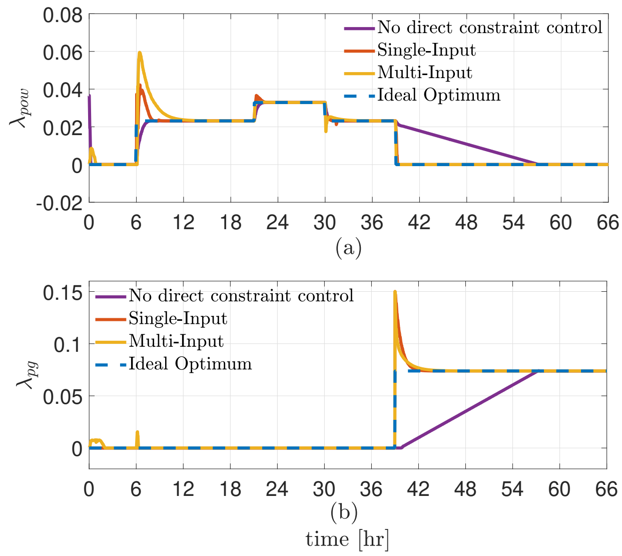

Fig. 7. The comparison of the Lagrange multiplier of the single-input, multi-input, primal-dual, and ideal optimum approaches.

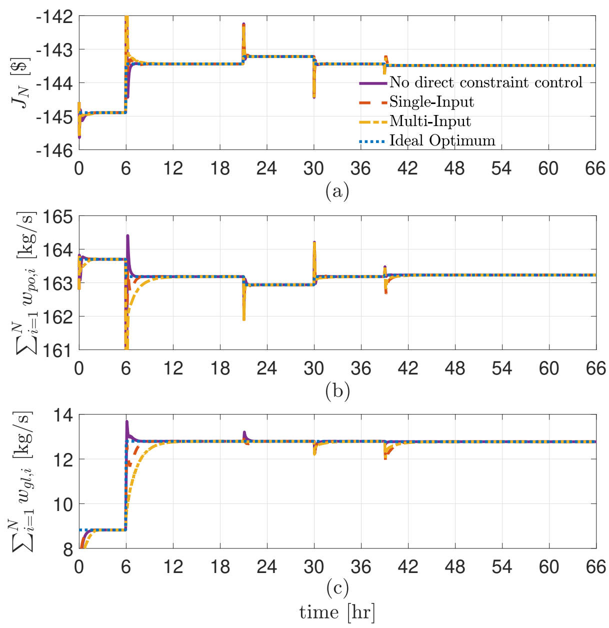

Fig. 8. The overall performance of the multi-input approach compared to the single-input, primal-dual, and ideal optimum

Krishnamoorthy, D. (2021). A distributed feedback-based online process optimization framework for optimal resource sharing. *Journal of Process Control*, 97, 72–83.

Krishnamoorthy, D., Jahanshahi, E., and Skogestad, S. (2019). A feedback real time optimization strategy using a novel steady-state gradient estimate and transient measurements. *Ind. Eng. Chem. Res.*, 58, 207—-216.

Krishnamoorthy, D. and Skogestad, S. (2022). Real-time optimization as a feedback control problem – a review. *Computers & Chemical Engineering*, 161, 107723.

Morari, M., Arkun, Y., and Stephanopoulos, G. (1980). Studies in the synthesis of control structures for chemical processes: Part i: Formulation of the problem. process decomposition and the classification of the control tasks analysis of the optimizing control structures. *AIChE Journal*, 26, 220 – 232.

Skogestad, S. (2003). Simple analytic rules for model reduction and pid controller tuning. *Journal of Process Control*, 13, 291–309.

Srinivasan, B., François, G., and Bonvin, D. (2011). Comparison of gradient estimation methods for real-time optimization. In *21st European Symposium on Computer Aided Process Engineering-ESCAPE 21*, 607–611.

Wenzel, S., Paulen, R., Stojanovski, G., Kramer, S., Beisheim, B., and Engell, S. (2016). Optimal resource allocation in industrial complexes by distributed optimization and dynamic pricing. *Automatisierungtechnik*, 64(6), 428–442.